Development of highly nano-dispersed NiO/GDC catalysts from ion exchange resin templates

A. Caravaca[*a,b] S. Picart,[c] M. Aouine,[b] B. Arab-Chapelet,[a] P. Vernoux,[b] and T. Delahaye[*a]

[a]CEA, DEN, DMRC/SFMA/LPCA, F-30207 Bagnols-sur-Cèze Cedex, France.

[b]Université de Lyon, CNRS, Université Claude Bernard Lyon 1, IRCELYON, UMR 5256, 2 avenue A. Einstein, 69626 Villeurbanne, France

[c]CEA, DEN/DMRC/CETAMA, F-30207 Bagnols-sur-Cèze Cedex, France

E-mail: angel.caravaca@cea.fr, thibaud.delahaye@cea.fr

1. Materials and methods

1.1. Precursors

A poly-acrylic resin (Dow Chemicals) was used as ion exchange template. It consists of IMAC HP333 gel type acrylic exchanger in the form of micro-spherical beads. Prior to be used, the resin was washed with a nitric acid 1 M solution (prepared from concentrated 64 % HNO_3, Fisher Chemical solutions, respectively), and then it was pretreated with ammonia 1 M solution (prepared from concentrated 25 % NH_3, Merck, Pro Analysis). This way, the resin had available NH_4^+ ions for exchange with the desired cations. Previous studies have demonstrated that for acrylic resin, the exchange capacity is pH dependent, and the reaction is only relevant when pH > 4 [1-3]. Hence, the presence of NH_4^+ ions (when released by the resin by ionic exchange) leads to a buffering effect, allowing to control the pH.

$Ce(NO_3)_3$ x 6 H_2O, (99.99 % purity, Merck), $Gd(NO_3)_3$ x 6 H_2O (99.9 % pure, Prolabo) and $Ni(NO_3)_2$ x 6 H_2O were used for the preparation of the starting solutions for resin loading.

1.2. Metal loading of the resin

Samples were prepared by the so-called Weak Acid Resin (WAR) method [1-6]. A first series of 6 materials was prepared. For each one, 8 mL of resin in the NH_4^+ form were poured into a beaker. In parallel, 100 mL solutions were prepared with different concentrations of Ni, Ce and Gd from the nitrate precursors. The solutions were prepared in a way that the Ce/Gd molar ratio was constant in all of them and equal to 4. Then, the Ni molar concentration was varied from 0 to 100 %. Samples were called: GDC, NiGDC X (X = 25, 50, 75, 90, being X the % mol Ni in starting solution), and 100 Ni (100 % Ni). Assuming an exchange capacity of the resin of 2.6 meq/mL$_{resin}$, the volume of the solutions for exchange was selected to have a 3 times excess of meq of cations in solution. The selected exchange time was 24 hours, in order to ensure equilibrium in the ionic exchange procedure. After loading, the resin was dried in an oven at 383 K overnight.

Then, in order to obtain the desired NiO/GDC catalysts, the dried resin was calcined in a static furnace. This way, as demonstrated in the above referenced studies, the organic skeleton of the resin will be gasified into CO, CO_2 and H_2O, leaving a mixture of the metal oxides. The calcination procedure followed was:

a) 25 - 150 ºC: 2 ºC / min
b) 150 - 450 ºC: 1 ºC / min (Resin calcination)
c) 450 ºC - 750 ºC: 2 ºC / min (Solid solution CeO_2/Gd_2O_3)
d) 750 ºC: 1 hour

Step b) allowed to slowly gasify the resin, avoiding an aggressive escape of CO_2 gas, and step c) allows to achieve a temperature high enough to ensure the solid CeO_2/Gd_2O_3 solid solution [3].

A second series of materials was prepared, in order to enhance the Specific Surface Area (SSA) of a selected material of the first series. First, 40 mL of resin in the NH_4^+ form were poured into a beaker. Then, a sample NiGDC90 (90 % mol Ni in starting solution) was prepared following the whole procedure above described (including exchange, drying and calcination). Using this catalyst as starting material, a series of new materials were prepared

by the partial dissolution of NiO, following a procedure already patented by Delahaye et al. [4]. 4 new samples were prepared. They were named Dis 25, Dis 50, Dis 75 and Dis 100, in which a stoichiometric amount of HNO_3 was added to dissolve 25, 50, 75 and 100 % of the NiO in the starting material (NiGDC90). The partial dissolution was performed at 90 °C for 12 hours. The obtained materials were vacuum-filtered and thoroughly washed with deionized water and dried overnight at 383 K.

1.3. Standard characterizations

The chemical composition of the materials after calcination was determined by ICP-AES analysis. Two different procedures were carried out to ensure consistency and reproducibillity of the obtained results:

1) First, a small amount of the solid materials after calcination was dissolved in two steps: a) by adding 5 mL of HNO_3 solution 4 M for 2 hours, and b) by adding 5 mL of H_2O_2 0.5 M and HNO_3 4 M solution for 12 hours. The solutions obtained were then analyzed by ICP-AES.
2) Secondly, the liquid solutions before (starting solution) and after exchange were analyzed by ICP-AES. The amount of metal in the resin and therefore in the final oxide materials was calculated by subtraction.

Regarding the second series of experiments, the catalysts obtained after the partial NiO dissolution in the starting material (NiGDC90) were dissolved and analyzed following the above described procedure (1). In addition, the HNO_3 solutions after partial dissolution of NiO were analyzed by ICP-AES.

Thermogravimetric (TGA) and differential scanning calorimetry (DSC) analysis were performed to identify the key temperatures and temperature ranges corresponding to the departure of H_2O and organic matter (acrylic skeleton) of the metal-loaded resin. A STA 449C Netzch equipment was used. The metal-loaded resin was placed in an alumina crucible and heated up to 1073 K at a heating rate of 2 K min^{-1}, under 20 mL min^{-1} of flowing air.

X-Ray Diffractometry (XRD) measurements were performed on the materials obtained after calcination (first series) and after partial NiO dissolution (second series). A Bruker D8 Advance apparatus was used, equipped with a Cu Ka1.2 radiation and a linear Lynx-Eye detector, in a θ–θ Bragg-Brentano configuration. The step was 0.02 °, with a step time of 0.2 s, from 20 to 60 °C. The refinement of the lattice parameters was carried out by Le Bail method using the "pattern matching" option of the TOPAS software (TOtal Pattern Analysis Solutions) from BRUKER AXS [1], where only the profile parameters (cell dimensions, peak shapes, background, zero point correction) were refined. The microstrains and average crystallite sizes were calculated with the fundamental parameters method [2]. The percent of microstrains in a structure can increase with incorporation of impurities in the cell or substitution of atoms.

---

[1] DIFFRACplus TOPAS/TOPAS R/TOPAS P Version 2.1 and www.bruker-axs.com.
[2] R.W. Cheary, A.A. Coelho, J.P. Cline, Fundamental parameters line profile fitting in laboratory diffractometers, J. Res. Natl. Inst. Stand. Technol. 109 (2004) 1–25.

BET method was used to measure the specific surface area of the catalysts. A Micromeritics Gemini 2360 Surface Area Analyzer with N_2 was used. The samples were outgassed under vacuum at room temperature for 12 hours, and then at 120 °C for 2 hours, before start the measurements.

A Ly-EtTEM microscope was used to visualize the nano-structure of a selected catalyst after partial NiO dissolution. It consists of a latest generation ETEM (Titan 80–300 kV from FEI™) equipped with an imaging aberration corrector and an energy-dispersive X-ray (EDX) analyzer (SDD X-Max 80 mm2 from Oxford Instruments™) used for elemental chemical analysis. The sample was deposited on titania grids covered with a silica film and placed into a Gatan™ furnace-type holder. The ETEM was operated with a beam voltage at 80 and 300 kV to evaluate the effect of the electron beam energy. Samples were observed under electron beam (irradiation, beam on) and without electron beam (beam off).
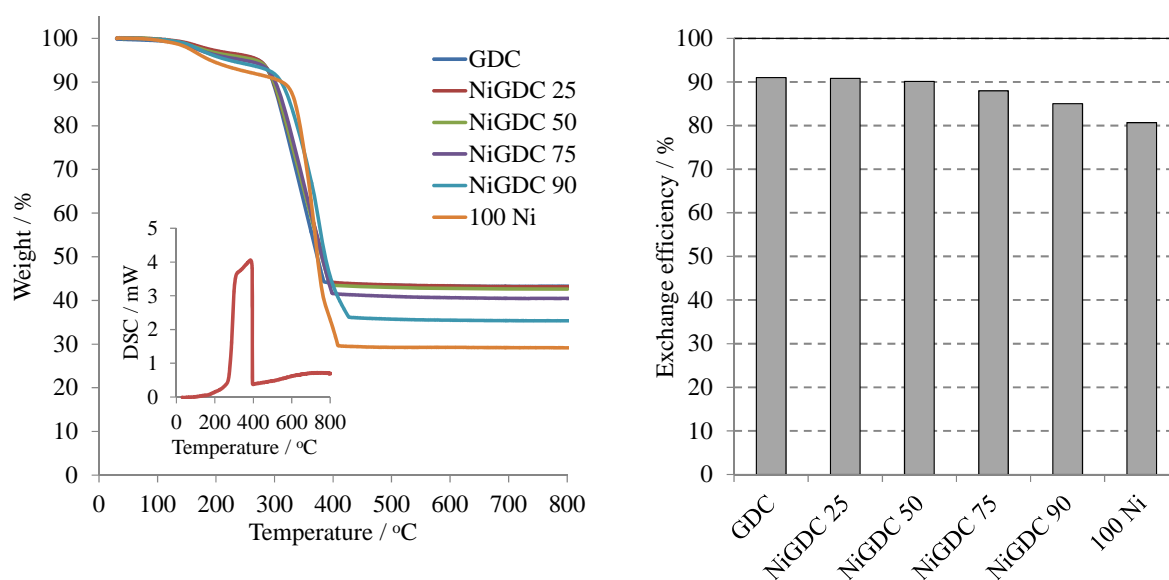
Results and discussion

Figure S1. (a) Thermogravimetric analysis of the first set of loaded resin materials performed under air (20 mL min^{-1}), showing the weight loss of the loaded resin as a function of temperature. Inset figure shows, as an example, the DSC analysis of the NiGDC 25 sample (with 25 % mol/mol Ni in the starting solution); (b) ***Exchange efficiency****, calculated on the basis of the TGA and ICP-AES results.

*Calculation Exchange Efficiency**

From ICP-AES analysis, we know mol% of Ce, Gd and Ni, just considering the metals:

$$mol\% \, Ce = \frac{mol \, Ce}{mol \, Ce + mol \, Gd + mol \, Ni} \quad [1]$$

$$mol\% \, Gd = \frac{mol \, Gd}{mol \, Ce + mol \, Gd + mol \, Ni} \quad [2]$$

$$mol\% \, Ni = \frac{mol \, Ni}{mol \, Ce + mol \, Gd + mol \, Ni} \quad [3]$$

The theoretical value of weight percentage of all metals exchanged in the dried resin corresponding to a full exchange is [2]:

$$Theoretical\ wt\%\ metal = \frac{MW_{metals\ exchanged}}{(MW_{metals\ exchanged} + MW_R)}\ [4]$$

With MWmetals exchanged being the molecular weight of the metals exchanged in the resin (Ce, Gd and Ni in this case), and R the carboxylic inorganic group in its deprotonated form. Combining equations 1-4, we can calculate the **"theoretical wt% metal"** as:

$$Theoretical\ wt\%\ metal$$
$$= \frac{MW_{Ce} \times \%\ mol\ Ce + MW_{Gd} \times \%\ mol\ Gd + MW_{Ni} \times \%\ mol\ Ni}{(3 \times 74 + MW_{Ce}) \times \%\ mol\ Ce + (3 \times 74 + MW_{Gd}) \times \%\ mol\ Gd + (2 \times 74 + MW_{Ni}) \times \%\ mol\ Ni}\ [5]$$

Now, to calculate the real wt% metal exchanged in the dried resin, we will use the results from TGA and ICP-AES analysis.

From TGA, we know that: wt% residue = wt% oxide $NiO/Ce_{1-x}Gd_xO_{2-x/2}$ [6]

From ICP we can also re-calculate the wt% of CeO_2, Gd_2O_3 and NiO in the oxides:

$$wt\%\ CeO_2 = \frac{mass\ CeO_2}{mass\ CeO_2 + mass\ Gd_2O_3 + mass\ NiO}\ [7]$$

$$wt\%\ Gd_2O_3 = \frac{mass\ Gd_2O_3}{mass\ CeO_2 + mass\ Gd_2O_3 + mass\ NiO}\ [8]$$

$$wt\%\ NiO = \frac{mass\ NiO}{mass\ CeO_2 + mass\ Gd_2O_3 + mass\ NiO}\ [9]$$

With wt% oxide (TGA, equation 6) and wt% of each oxide (ICP, equations 7-9), we calculate the individual percentage of each oxide after the TGA:

$$wt\%\ CeO_2\ after\ TGA = wt\%\ oxide \times wt\%\ CeO_2\ [10]$$
$$wt\%\ Gd_2O_3\ after\ TGA = wt\%\ oxide \times wt\%\ Gd_2O_3\ [11]$$
$$wt\%\ NiO\ after\ TGA = wt\%\ oxide \times wt\%\ NiO\ [12]$$

Using results from equations 10-13, we can calculate the wt% of each metal after TGA by using the gravimetric factor:

$$wt\%\ Ce\ after\ TGA = wt\%\ CeO_2\ after\ TGA \times \frac{MW_{Ce}}{MW_{CeO_2}}\ [13]$$

$$wt\%\ Gd\ after\ TGA = wt\%\ Gd_2O_3\ after\ TGA \times 2 \times \frac{MW_{Gd}}{MW_{Gd_2O_3}}\ [14]$$

$$wt\%\ Ni\ after\ TGA = wt\%\ NiO\ after\ TGA \times \frac{MW_{Ni}}{MW_{NiO}}\ [15]$$

With results from equations 13-15, we can calculate the real wt% metal exchanged in the dried resin as:

$$Real\ wt\%\ metal = wt\%\ Ce\ after\ TGA + wt\%\ Gd\ after\ TGA + wt\%\ Ni\ after\ TGA \quad [16]$$

Therefore, combining the results from equations 5 and 16, the exchange efficiency will be:

$$\%\ Exchage\ efficiency = \frac{Real\ wt\%\ metal}{Theoretical\ wt\%\ metal} \times 100$$

Table S1. Lattice Parameters, crystallite size and strain of GDC and NiO, for the 1st and 2nd series of catalysts, based on the XRD measurements.

|		GDC			NiO					
		a (Å)	Cristallite size (nm)	strain	a (Å)	b (Å)	c (Å)	b(°)	Cristallite size (nm)	strain
1st series of catalysts WAR	GDC	5.4280(1)	31(1)	0.39(1)						
	NiGDC 25	5.4268(2)	25(1)	0.53(1)						
	NiGDC 50	5.4261(2)	24(1)	0.51(1)						
	NiGDC 75	5.4251(2)	18(1)	0.65(1)						
	NiGDC 90	5.4235(6)	10(1)	0.96(3)	5.114(2)	2.948(1)	2.988(1)	125.39(2)	11(1)	0.42(15)
2nd series of catalysts WAR + NiO dissolution	NiGDC 90	5.4237(8)	10(1)	0.85(5)	5.086(3)	2.947(2)	2.987(2)	125.20(4)	13(1)	0.97(14)
	Dis 25	5.4222(4)	10(1)	0.97(4)	5.156(6)	2.903(1)	2.979(1)	125.51(8)	10(1)	0.62(15)
	Dis 50	5.4214(6)	11(1)	1.05(3)	5.067(2)	2.939(2)	2.985(1)	125.53(4)	11(1)	0.75(11)
	Dis 75	5.4246(5)	11(1)	0.94(3)	5.065(4)	2.994(8)	2.934(2)	125.65(6)	13(1)	1.03(90)
	Dis 100	5.4244(5)	11(1)	0.97(2)						
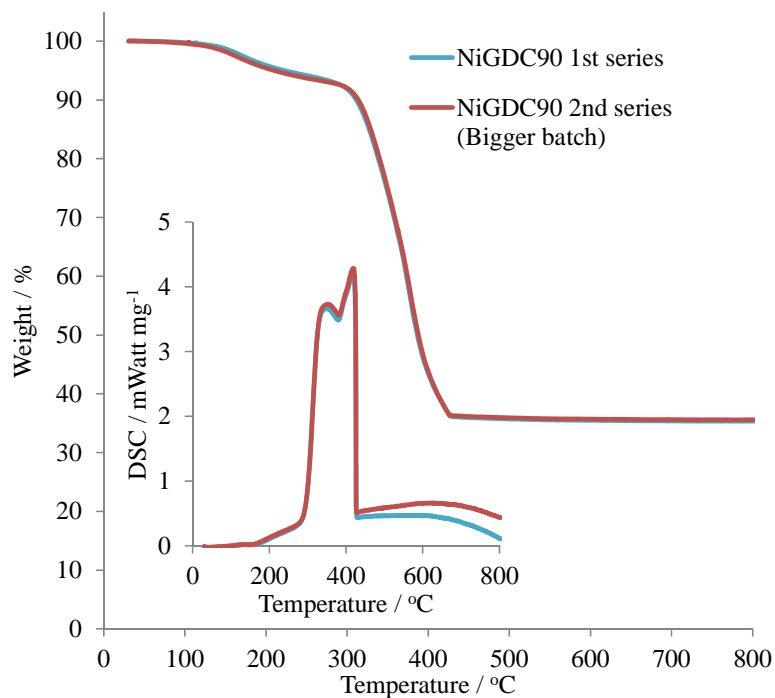
Figure S2. a) Thermogravimetric analysis of the sample NiGDC 90 prepared in the first series of loaded resin materials, and the sample NiGDC 90 prepared for the second series of catalysts. Both experiments were performed under air (20 mL min^{-1}). 8 mL and 40 mL of NH_4^+ resin were exchanged, respectively, with solutions containing Ni, Ce and Gd (see ESI†, section 1.2). Inset figure shows the DSC analysis for both samples.

Table S2. % mol/mol Ni and % w/w of Ni (if it was reduced) according to ICP-AES analysis, and Specific Surface Area (BET) of the catalysts after calcination of the loaded resin.

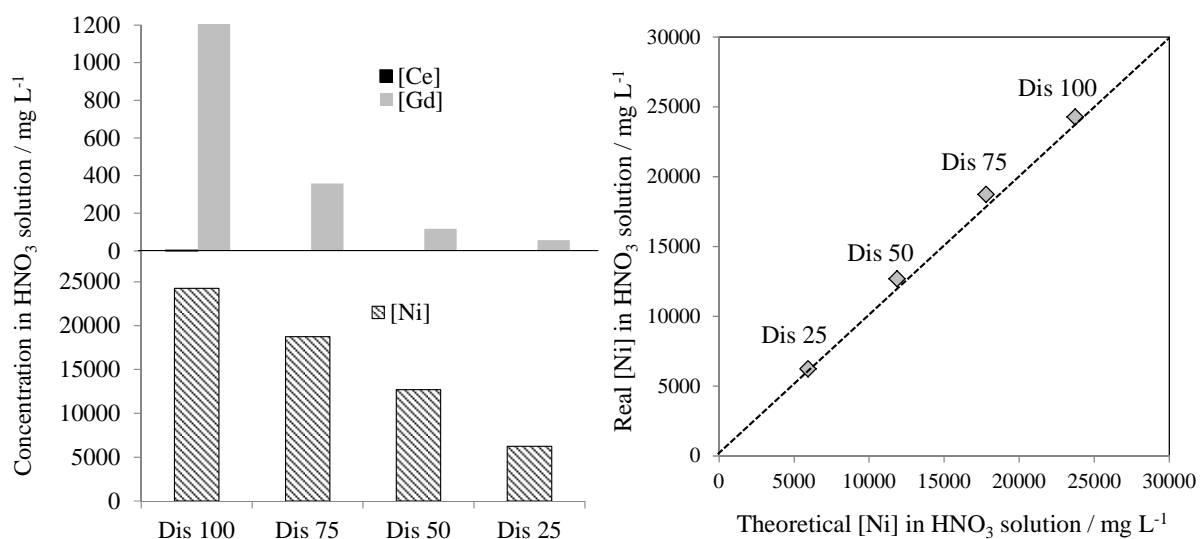|	% mol/mol Ni mol Ni/mol Ce+Gd+Ni	% w/w Ni reduced mg Ni/(mg Ni +mg CeO₂+mg Gd₂O₃)	Specific Surface Area / m² g⁻¹
NiGDC90 1st series	66.2	39.8	26
NiGDC90 2nd series	63.8	37.3	25

Figure S3. a) ICP-AES analysis of the second series catalysts after the NiO partial dissolution regarding the concentration of Ce, Gd and Ni in the HNO_3 solution used to dissolve NiO; b) Comparison of Ni concentration in the HNO_3 solution after partial dissolution, and the theoretical amounts expected, considering stoichiometric dissolution of NiO with HNO_3.
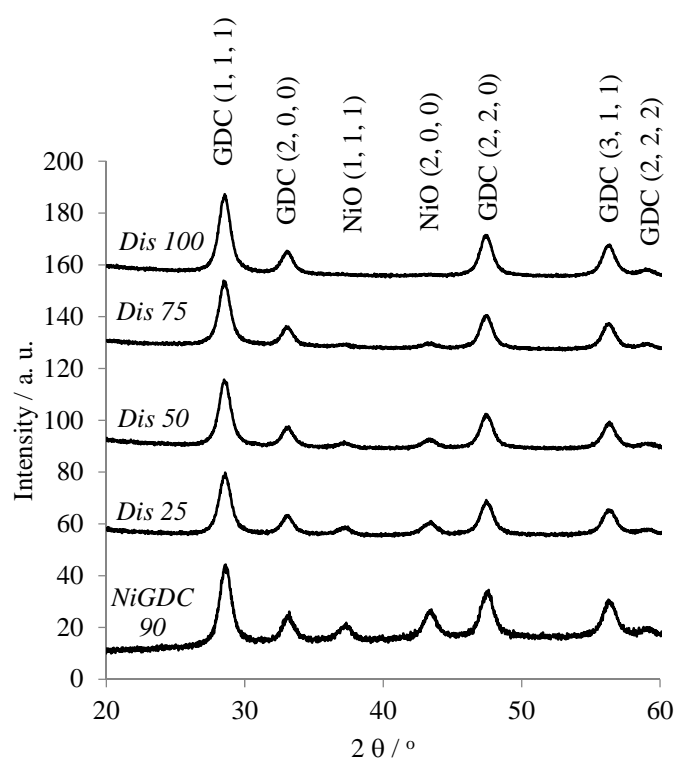

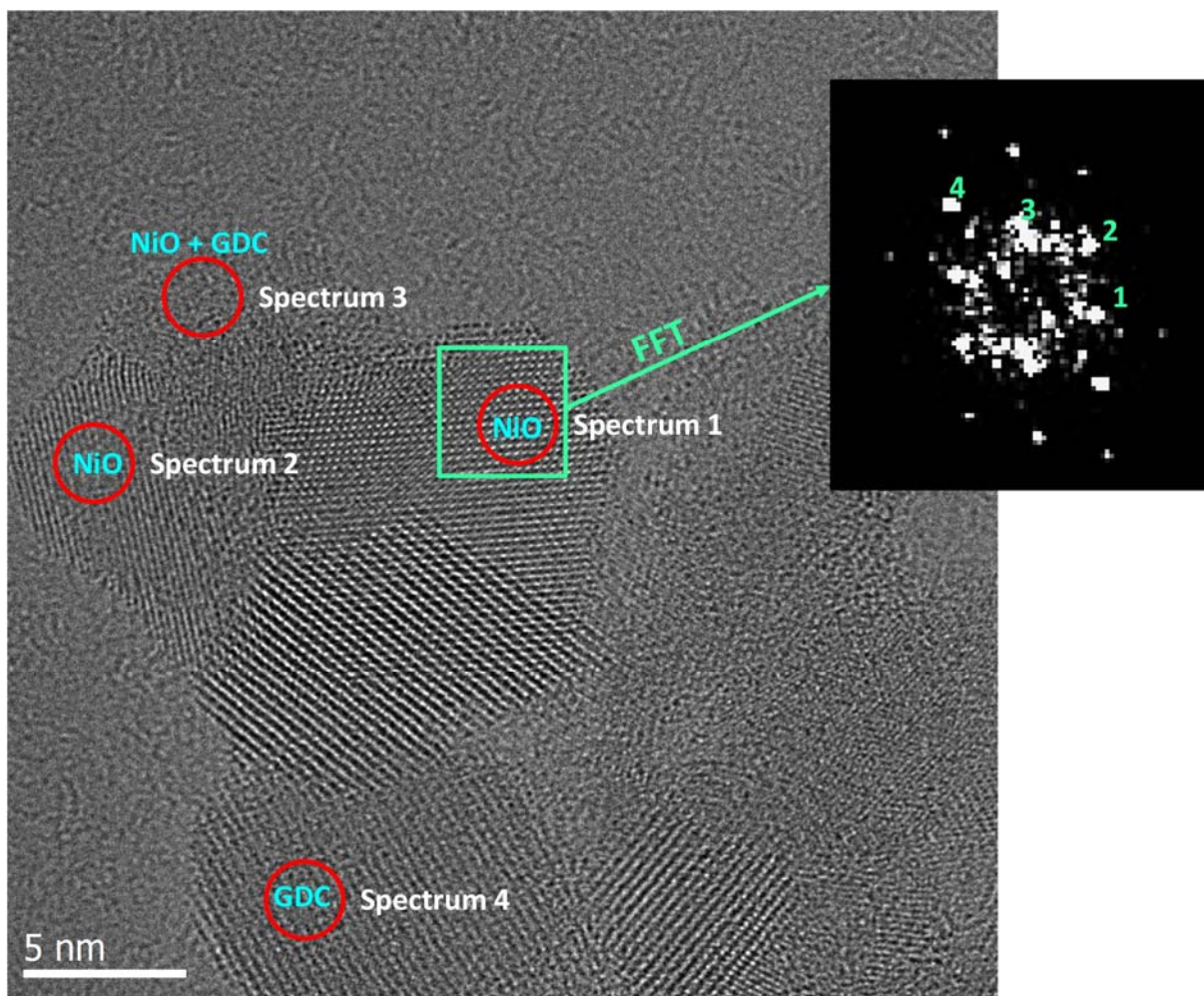Figure S4. XRD patterns of the second series of catalysts after the NiO partial dissolution.

Figure S5. TEM image of catalyst Dis 50 (50 % of Ni in starting material, NiGDC 90, was selectively dissolved)

Table S3. Fast Fourier Transform (FFT) analysis of selected area on Figure S5. The experimental results were compared with a theoretical cubic NiO crystal structure *(Reference code: 03-065-5745, Space group: Fm-3m (225), a (Å) = 4.1770)*. In this table it could be observed that both, theoretical and experimental analysis totally matched, confirming the nature and the presence of NiO nanoparticles, in this case with a size ~ 5 nm.

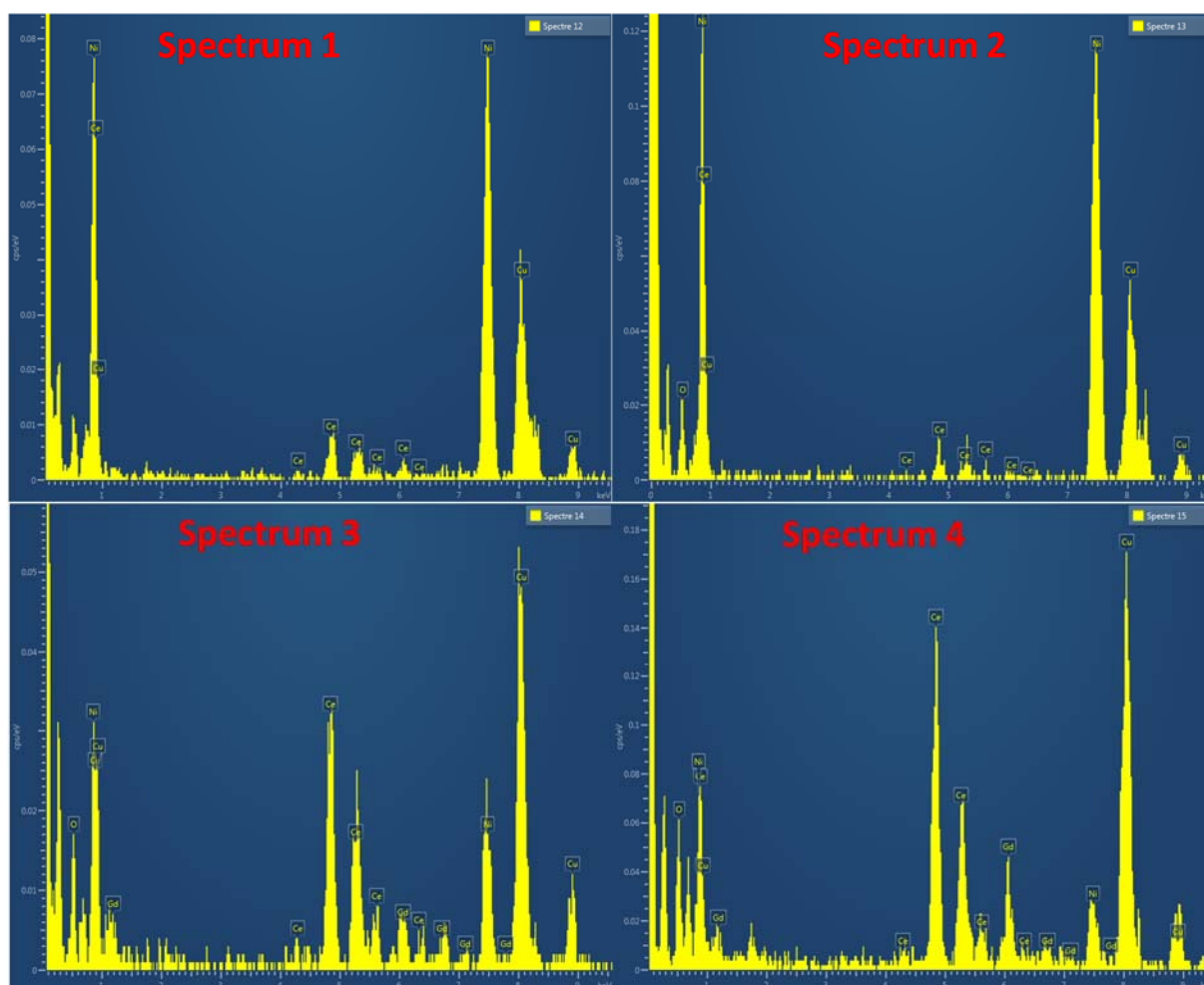| Spot n°	h k l	d(experimental) nm	α(experimental)	d(theoretical) nm	α(theoretical)
1	1 1 -1	0.2371	0.00	0.2412	0.00
2	2 0 0	0.2118	55.03	0.2089	54.74
3	1 -1 1	0.2389	110.11	0.2412	109.47
4	0 -2 2	0.1460	145.01	0.1477	144.74

Figure S6. EDX analysis of the areas highlighted on Figure S5. It confirms the nature and distribution of NiO and GDC nanoparticles, all of them with a particle size < 8 nm.

1. S. Picart, P. Parant, M. Caisso, E. Remy, H. Mokhtari, I. Jobelin, J. P. Bayle, C. L. Martin, P. Blanchart, A. Ayral and T. Delahaye, *The European Physical Journal Special Topics*, 2015, **224**, 1675-1687.
2. E. Remy, S. Picart, S. Grandjean, T. Delahaye, N. Herlet, P. Allegri, O. Dugne, R. Podor, N. Clavier, P. Blanchart and A. Ayral, *Journal of the European Ceramic Society*, 2012, **32**, 3199-3209.
3. M. Caisso, F. Lebreton, D. Horlait, S. Picart, P. M. Martin, R. Bès, C. Renard, P. Roussel, D. R. Neuville, K. Dardenne, J. Rothe, T. Delahaye and A. Ayral, *Journal of Solid State Chemistry*, 2014, **218**, 155-163.
4. T. Delahaye, M. Caisso, S. Picart, French Patent, EP3034483 A1, 2016.
5. M. Caisso, R. Boulesteix, S. Picart, A. Maître, T. Delahaye and A. Ayral, *Journal of the American Ceramic Society*, DOI: 10.1111/jace.14993, n/a-n/a.
6. T. Delahaye, M. Caisso, S. Picart, French Patent, EP3034209 A1, 2016.